Electronic conduction in $LaNiO_{3-\delta}$: the dependence on the oxygen stoichiometry δ

1998 J. Phys.: Condens. Matter 10 1323

(http://iopscience.iop.org/0953-8984/10/6/015)

J. Phys.: Condens. Matter **10** (1998) 1323–1338. Printed in the UK PII: S0953-8984(98)87384-0

Electronic conduction in $LaNiO_{3-\delta}$: the dependence on the oxygen stoichiometry δ

N Gayathri†§, A K Raychaudhuri†‖, X Q Xu‡, J L Peng‡ and R L Greene‡

† Department of Physics, Indian Institute of Science, Bangalore 560012, India

‡ Center for Superconductivity Research, University of Maryland, College Park, MD 20742, USA

Received 8 September 1997

Abstract. We report a systematic study of the electronic transport properties of the metallic perovskite oxide $LaNiO_{3-\delta}$ as a function of the oxygen stoichiometry δ ($\delta \leqslant 0.14$). The electrical resistivity, magnetoresistance, susceptibility, Hall effect and thermopower have been studied. All of the transport coefficients are dependent on the value of δ. The resistivity increases almost exponentially as δ increases. We relate this increase in ρ to the creation of Ni^{2+} with square-planar coordination. We find that there is a distinct $T^{1.5}$-contribution to the resistivity over the whole temperature range. The thermopower is negative, as expected for systems with electrons as the carrier, but the Hall coefficient is positive. We have given a qualitative and quantitative explanation for the different quantities observed and their systematic variation with the stoichiometry δ.

1. Introduction

Electrical conduction in transition metal perovskite oxides at low temperatures is a topic of intense current interest [1]. Most of these oxides belong to the class of ABO_3 or its closely linked derivatives. The interest in these materials has arisen because a number of different phenomena (such as ferroelectricity, superconductivity, metal–insulator transitions and giant magnetoresistance) can be seen in these materials. Many oxides of ABO_3 structure with the B ion belonging to the 3d transition metal group and a divalent ion like Sr or Ca at the A site are metallic [2]. In this case the B ions have a formal valency of 4+. One notable exception is the well known ferroelectric $SrTiO_3$ (a band insulator with an empty 3d band). On the other hand, when A is a trivalent cation like La or Pr, B cations have a formal valency of 3+. It turns out that almost all such oxides with the B cation in a trivalent state are insulating except $LaNiO_3$ [3–9] and $LaCuO_3$ [10]. $LaNiO_3$ is a fairly good metal with low resistivity although Ni has a formal valency of 3+. Technologically, $LaNiO_3$ is an interesting material because of its potential application in metallic interconnects (or electrodes) in thin-film oxide electronic devices, particularly those needing epitaxial multilayer perovskite oxide films [11]. $LaNiO_3$ has a pseudo-cubic structure with a small rhombohedral distortion. Its unit cell (containing two formula units) can be mapped onto a primitive rhombohedral cell with the pseudo-cubic lattice constants a (cell edge) $= 3.838$ Å and α (angle) $= 90^\circ 40'$ (for a perfect cube $\alpha = 90^\circ$; the rhombohedral distortion, $\alpha - 90^\circ \approx 40'$, is thus small). For

§ E-mail: gayathri@physics.iisc.ernet.in.

‖ E-mail: arup@physics.iisc.ernet.in.

0953-8984/98/061323+16$19.50

details of the structural data, see reference [4] and reference [12]. Like many perovskite oxides belonging to this class, the material has a tendency to lose oxygen, leading to the creation of Ni^{2+} ions. This is particularly critical at higher temperatures where, by loss of oxygen, it tends to become La_2NiO_4 which has K_2NiF_4 structure. In $LaNiO_{3-\delta}$, Ni is octahedrally bonded to six oxygen atoms when δ is low. In La_2NiO_4 the bonding of Ni^{2+} has a square-planar form. The change of bonding on formation of Ni^{2+} (as δ is increased) has important implications as regards the physical properties of this material. In this paper we focus on this particular aspect of oxygen stoichiometry and show that fixing oxygen in $LaNiO_{3-\delta}$ is crucial for the determination of such important quantities as the resistivity (ρ), magnetoresistance (MR) and thermopower (S). For instance, ρ can change by an order of magnitude or more when δ deviates from zero by as little as 0.1. We discuss the likely origin of this behaviour in this paper.

Table 1. Different physical quantities obtained from low-temperature experiments as reported by various groups.

	$\rho_{300\,K}$ ($\mu\Omega$ cm)	$\Delta\rho$† ($\mu\Omega$ cm)	A‡ ($\mu\Omega$ cm K^{-2})	S(300 K) (μV K^{-1})	(dS/dT)(300 K) (μV K^{-2})	γ_{sp}§ (mJ mol^{-1} K^{-2})	χ_0¶ (emu mol^{-1})
Rajeev *et al* [4]	1700	1133	0.003	−18	−0.052 23	15	—
Sreedhar *et al* [5]	2150	1702	0.034	—		14	5.1×10^{-4}
Xu *et al* [6]	380	345	0.006	−22	−0.0490	—	4.9×10^{-4}

† $\Delta\rho = \rho_{300\,K} - \rho_{4.2\,K}$.
‡ The coefficient of the T^2-term at low temperature.
§ The linear term in the low-temperature specific heat.
¶ The temperature-independent magnetic susceptibility.

In the past, there have been quite a few studies [3–6] on the electronic transport and thermodynamic properties of $LaNiO_{3-\delta}$. In table 1 we summarize the main results of some of the past investigations which reported the temperature dependence of the resistivity [4–7]. This table also includes the temperature-independent Pauli-like paramagnetic susceptibility measured by different groups [5, 6]. It can be seen that the absolute value of ρ as well as its temperature dependence (quantified by $\Delta\rho(300\ K) = \rho(300\ K) - \rho(4.2\ K)$) vary widely from one investigation to another. While it was believed that the oxygen stoichiometry (i.e., $\delta \neq 0$) may be the origin of these differences, no systematic investigation has been made to establish this quantitatively. From our investigation, presented below, we establish that most of the differences seen in table 1 do indeed arise from the differences in the oxygen stoichiometry.

We also perform a systematic investigation of the temperature dependence of ρ in order to find the different terms which contribute to $\rho(T)$. We find that there exists an unambiguous $T^{1.5}$-contribution to $\rho(T)$. In contrast to previously published results [4–6] our findings are that there may or may not exist a T^2-term in the resistivity which can be connected to electron correlation effects. In particular we show that the coefficient of the T^2-term (even if it exists) is strongly dependent on δ. As a result one has to exercise caution if any intrinsic origin is to be assigned to it. In table 1, we also show the thermopower (S). The thermopower reported by all of the groups is negative and linear over an extensive temperature range. The negative thermopower of $LaNiO_3$ implies an electron-like nature for the charge carriers. To further investigate the nature of the charge carrier in $LaNiO_3$

we made a Hall measurement on thin films of this material. Interestingly, we find that the Hall coefficient is positive over the whole temperature range, confounding the naive expectations from the negative Seebeck effect. We discuss the implications of this rather intriguing observation.

2. Experimental details

The samples of $LaNiO_{3-\delta}$ were prepared by decomposition of co-precipitated nitrates of La and Ni as described in detail in reference [13] and reference [6]. Weighed quantities of the parent compounds, La_2O_3 and nickel oxalate, were dissolved in concentrated nitric acid and the solution was evaporated until the nitrate mixture precipitated. This nitrate mixture was decomposed at 450 °C in air. The mixture was repeatedly ground, pelletized and heat treated at 950 °C in an oxygen atmosphere. The final heat treatment was given at 1000 °C for varying durations in an oxygen atmosphere. The best oxygen stoichiometry ($\delta \approx 0$) was obtained by high-pressure (195 bar) oxygen annealing at 1000 °C for 70 h. The samples produced by the above method were x-rayed to check for phase purity and also to measure the lattice constants. The grain sizes of the samples were measured using a scanning electron microscope. The grain sizes were typically of the order of 1–2 μm. The oxygen stoichiometry δ was determined by iodometric titration. The Hall coefficient and thermopower measurements were made on a film of $LaNiO_3$ deposited by pulsed laser ablation on a $LaAlO_3$ substrate. The substrate temperature was maintained between 700 °C and 800 °C and the oxygen partial pressure was around 700 mbar during the film growth. The thickness of the film obtained was around 2000 Å.

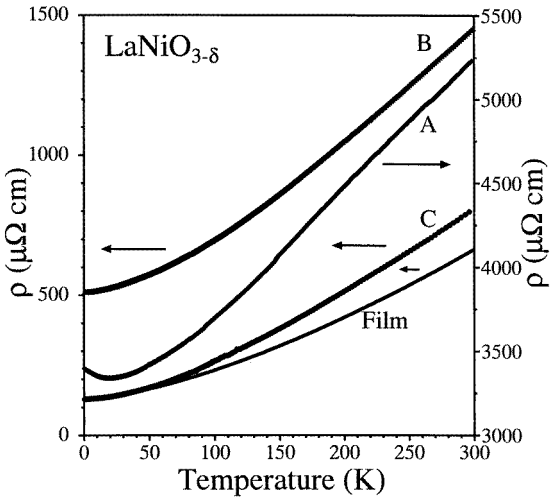

Figure 1. The resistivities (ρ) of the three samples of $LaNiO_{3-\delta}$. The samples A, B and C have $\delta = 0.14$, 0.08 and 0.02 respectively. The resistivity of the $LaNiO_3$ film used for the measurement of the Hall constant and thermopower is also shown.

The electrical resistivity $\rho(T)$ was measured by a high-precision low-frequency (20 Hz) ac bridge technique in the range 0.4–300 K. The temperature range was covered by a combination of two cryostats. The Hall effect was measured down to 1.5 K in a field of 6 T. The thermopower was measured by a standard dc technique. We also obtained the

magnetic characterization by measuring the susceptibility (χ) using a SQUID magnetometer.

3. Results and discussion

3.1. The magnitude of the resistivity

In figure 1 we present the resistivity measurements for the three samples with the general formula $LaNiO_{3-\delta}$. In the same graph we show the data on the epitaxial film for which we have measured the Hall voltage and the thermopower.

Table 2. A summary of the results obtained from our experiment.

Sample	δ	$\rho_{300\,K}$ ($\mu\Omega$ cm)	$\rho_{4.2\,K}$ ($\mu\Omega$ cm)	ℓ_{el}† (Å)	MR‡ (%)	S (at 300 K) (μV K^{-1})	(dS/dT)(300 K) (μV K^{-2})
A	0.14	5350	3340	0.8	−0.28	−30	−0.040 39
B	0.08	1450	414	5	−0.04	−18	−0.048 17
C	0.02	790	130	15	0.9	—	—

† The elastic mean free path estimated from equation (1).
‡ The magnetoresistance at $T = 4.2$ K and 6 T.

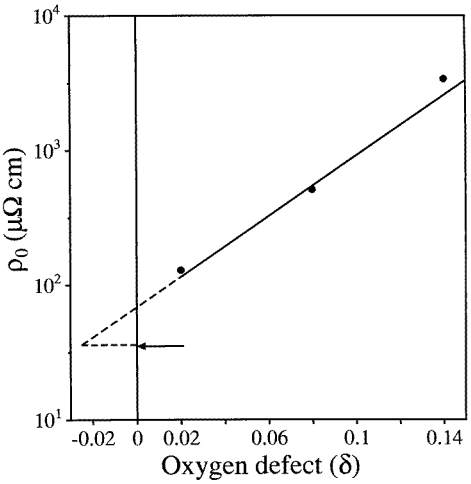

Figure 2. The zero-temperature resistivity (ρ_0) as a function of the oxygen defect δ. The arrow marks the ρ_0-value reported in reference [6]

The relevant numbers, including δ as measured by titration, have been collected together in table 2. (*Note:* we identify the samples in decreasing order of δ and have called them A, B and C for $\delta = 0.14$, 0.08 and 0.02 respectively.) All of the sample $\rho(T)$ curves show a metallic behaviour although the residual resistivity ρ_0 increases by a factor of 30 as δ changes from 0.02 to 0.14. (This change in δ translates into a Ni^{2+} content $\approx 2\delta$.) For the samples in reference [6] $\rho_0 \approx 34$ $\mu\Omega$ cm which is about a factor of 3.9 lower than the lowest value of ρ_0 found for our samples. The dependence of ρ_0 on the oxygen content (δ) is shown in figure 2 where we plot ρ_0 as a function of δ. It can be seen that ρ_0 has an almost exponential dependence on δ. As δ increases, leading to an increase of Ni^{2+} concentration, we have a rapid increase in ρ_0 (see table 2).

The increase in ρ_0 does not scale with the reduction of carriers (we assume that Ni^{3+} only contributes itinerant carriers) but implies a strong reduction in the elastic mean free path with increase of the Ni^{2+} concentration. To quantify this with an approximate estimate we use the simple free-electron expression [14]

$$\ell_{el} = \frac{\hbar}{e^2}\frac{1}{\rho_0}\left(\frac{3\pi^2}{{n_e}^2}\right)^{1/3} \tag{1}$$

where ℓ_{el} is the elastic mean free path and n_e is the carrier concentration. The results obtained are shown in table 2. In $LaNiO_{3-\delta}$ ($\delta \approx 0$) the carrier density $n_e \approx 1.7 \times 10^{22}$ cm^{-3} assuming one carrier from each Ni^{3+}. (We will see later that this is very close to the estimate from our Hall measurement, $\approx 2 \times 10^{22}$ cm^{-3}). For $\delta > 0$, we assume that the Ni^{2+} created does not contribute carriers and this proportionately reduces the carrier density. For the sample with $\delta = 0.14$ which has the highest value of ρ_0, the mean free path (ℓ_{el}) is somewhat smaller than the Ni–O bond length ($\approx$2 Å) and we are at the limit of the metallic state. Interestingly, it can be seen that for this sample there is a resistivity minimum at around 20 K. We find that this arises from a weak-localization effect which is expected in this sample due to its short mean free path [14]. (*Note:* the above discussion on the mean free path is only approximate, since we used a simple free-electron expression.) In figure 2, we have indicated by a dotted line $\rho_0 \approx 34$ $\mu\Omega$ cm which is the lowest resistance reported for $LaNiO_{3-\delta}$ so far [6]. If the dependence of ρ_0 on δ persists down to the lowest δ, we can conclude that for this particular sample $\delta \approx -0.03$. However, for the ABO_3 structure one cannot admit oxygen in excess of 3. Thus a small $\delta \approx -0.03$ will imply a small number of cation vacancies leading to a relatively higher oxygen-to-cation ratio.

The important observation that emerges from our results is the strong dependence of ρ_0 on δ. For conventional metals and alloys the dependences of ρ_0 on the small number of impurities etc are rarely that strong. We think that this strong dependence depends on two factors: (i) the difference between the energies of the d levels of Ni^{2+} and Ni^{3+} and, more importantly, (ii) the change of Ni coordination from octahedral to square planar. The change of Ni from octahedral (as in $LaNiO_3$) to square-planar coordination (as in La_2NiO_4) occurs as more Ni^{2+} ions are created as δ is increased. For the square-planar coordination the transfer integral for electrons going from one site to another is severely decreased because Ni^{2+} takes a two-dimensional configuration. The square-planar configuration also introduces a large lattice strain. This strain distorts the existing NiO_6 octahedra, changing the Ni–O–Ni bond angle from 180° which in turn also reduces the hopping integral. We can think of this reduction in the hopping integral as a reduction of the effective bandwidth, thereby localizing the carriers within a length scale of one unit cell. As δ and hence the Ni^{2+} concentration increases further, the lattice becomes too unstable for octahedral coordination of Ni and stabilizes only via disordered intergrowths of octahedral and square-planar layers [12]. The material with intergrowths will then behave as a 'composite' of two materials having different resistivities. In short, the increase of ρ_0 on increase of δ therefore seems to be more influenced by the changes in the coordination of the Ni ion.

In polycrystalline oxide materials the grain boundary often has a different oxygen stoichiometry to the bulk. If the grain boundary contributes to the overall resistivity, then the stoichiometry of the grain boundary will be of importance. For this material we have reason to believe that whatever the mechanism is that is limiting the mean free path of the electron, it occurs in the bulk of the grain. The largest mean free path seen in these materials is $\approx$20 Å in the sample with lowest δ. Electron micrograph studies show that the typical grain size $\approx$1–2 μm. Thus, as the mean free path is much smaller than the grain size, we feel that the grain boundary contribution to ρ will not be of much significance.

Also, the grain sizes in all of the materials studied are similar since these materials have all been prepared with the same type of heat treatment. They differ only in the final oxygen annealing. The resistivities of the samples with low δ are very similar to the resistivity of the epitaxial film (see figure 1), providing further evidence of the insignificant role of grain boundaries.

3.2. The temperature dependence of ρ

The exact temperature dependence of $\rho(T)$ for metallic oxides like $LaNiO_3$ has not been critically looked into for samples with varying oxygen content. In particular, the temperature dependence of ρ has contributions arising from different sources. As we discuss below, the relative contributions of the different terms are strongly dependent on the oxygen stoichiometry. In the following we have taken a fresh look at this issue of temperature dependence with a view to obtaining a quantitative evaluation of the different contributions.

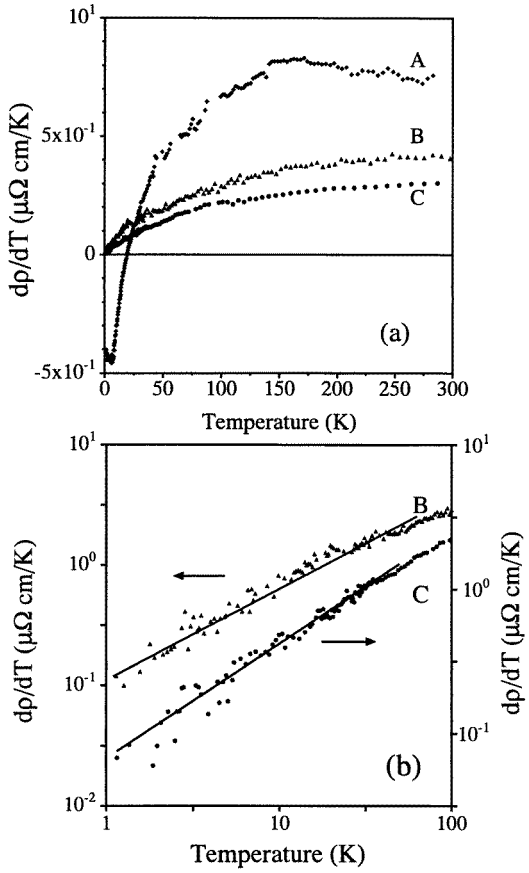

Figure 3. (a) $d\rho/dT$ as a function of T for samples A, B and C as a function of T for $0.4 \leqslant T \leqslant 300$ K. (b) A log–log plot of $d\rho/dT$ versus T for the temperature range $1.5 < T < 100$ K constructed to find out the leading power-law dependence of ρ on T at low temperature. The lines show the fits to the data up to $T = 50$ K.

A study of $d\rho/dT$ as a function of T often provides a rough guide to the leading

temperature-dependent terms of ρ. For samples B and C (which are less resistive), $d\rho/dT \to 0$ as $T \to 0$ implying that ρ reaches a residual resistivity (see figure 3(a)). At higher temperatures $T > 150$ K, $d\rho/dT$ is almost constant, showing the dominance of the linear temperature dependence of ρ. For sample A (which has the highest resistivity) $d\rho/dT = 0$ at a finite temperature (T_{min}) where ρ shows a minimum. For this sample $d\rho/dT$ is negative and finite as $T \to 0$. Due to the existence of the resistivity minima it is difficult to determine the limiting temperature dependence of ρ. However, this can be clearly established for samples B and C. In figure 3(b) we have plotted $d\rho/dT$ versus T on a log–log scale for $1.5 < T < 100$ K. $d\rho/dT$ follows a temperature dependence $\sim T^p$, where $p \approx 0.75 \pm 0.02$ for both samples. This implies that as $T \to 0$, $(\rho - \rho_0) \sim T^{1.75}$. As we will see below, this particular type of temperature dependence arises from a combination of a $T^{1.5}$-term and an additional T^n-term with $n \geqslant 2$. This particular form of $d\rho/dT$ clearly establishes that a single term (like a T^2-term) cannot explain the data and one needs at least two contributions with different temperature dependences.

Table 3. Results of the fit of the resistivity data to equations (2), (4) and (6).

$\rho = \rho_0 + \alpha T^{1.5} + \beta f_n[T] - \gamma T^{0.75}$								
Sample		Maximum error	Comments	ρ_0 ($\mu\Omega$ cm)	α ($\mu\Omega$ cm K$^{-1.5}$)	β ($\mu\Omega$ cm)	γ ($\mu\Omega$ cm K$^{-0.75}$)	θ_R (K)
A	$n = 2$	±0.7%	No systematic deviation†	3406	0.146	2234	10.97	340
	$n = 5$	±0.5%	No systematic deviation	511.45	0.156	500	—	250
B	$n = 3$	±1%	Systematic deviation at high T	511	0.162	250	—	300
	$n = 2$	±1%	Systematic deviation at high T	510	0.160	153	—	340
	$n = 5$	±0.5%	No systematic deviation	129	0.099	774	—	325
C	$n = 3$	±1%	Systematic deviation at low T	128	0.099	416	—	349.4
	$n = 2$	±2.5%	Systematic deviation at high T	126	0.115	109	—	340

† For $n = 3$ and $n = 5$ the error was in excess of ±1% and systematic deviation was observed. The error has been defined through equation (3).

We have used different strategies to obtain the best fit to the observed data. The various relations that we have used are shown in tables 3 and 4. In the following we present the main results only. For samples B and C which do not show any resistivity minima at low temperatures we use the following expression:

$$\rho(T) = \rho_0 + \alpha T^{1.5} + \beta f(T) \tag{2}$$

where ρ_0, α and β are fitting parameters. We find that a $T^{1.5}$-term is always necessary to fit the data over the whole temperature range. However, the $T^{1.5}$-term alone is not sufficient and we need an additional temperature-dependent term $f(T)$ which at $T < 50$ K has a temperature dependence $\sim T^n$ with $n \geqslant 2$ and for $T > 150$ K has a almost linear

Table 4. Results of the fit of the resistivity data to equations (2), (5) and (6). *Note:* no systematic deviation was observed in any of the fits. The error is defined through equation (3).

$\rho = \rho_c + \alpha' T^{1.5} + \beta' T^m - \gamma' T^{0.75}$						
Sample		Maximum error	ρ_c ($\mu\Omega$ cm)	α' ($\mu\Omega$ cm K$^{-1.5}$)	β' ($\mu\Omega$ cm K^{-m})	γ' ($\mu\Omega$ cm K$^{-0.75}$)
A	$m = 2$ ($T < 50$ K)	±0.2%	3409	0.403	0.045	12.95
	$m = 1$ ($T > 100$ K)	±0.3%	2828	−0.044†	8.8	—
B	$m = 2$ ($T < 50$ K)	±0.2%	511	0.148	0.0053	—
	$m = 1$ ($T > 100$ K)	±0.6%	426.6	0.105	1.64	—
C	$m = 2$ ($T < 50$ K)	±0.3%	129	0.0543	0.0087	—
	$m = 1$ ($T > 100$ K)	±0.6%	86	0.0879	0.891	—

† The negative α' is an artifact of the fitting procedure and has no physical significance. This arises because of the large $\beta' T^m$-term which makes the contribution from the $\alpha' T^{1.5}$-term negligible.

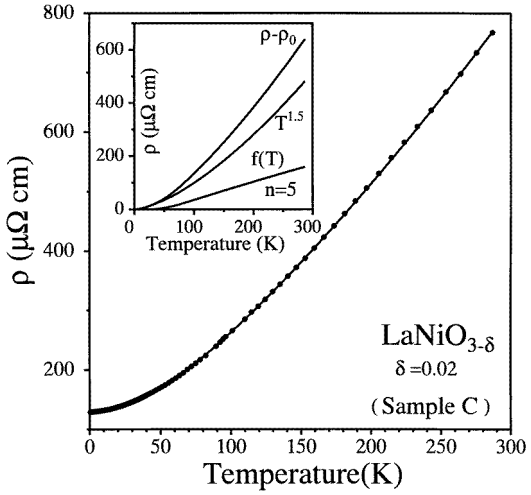

Figure 4. The data and fit for sample C as a function of temperature using equation (2) with $f_n(T)$ given by equation (4) ($n = 5$). Inset: the relative contributions of the different terms for the resistivity.

temperature dependence. The different forms of $f(T)$ as well as the results of the non-linear least-squares fits are summarized in tables 3 and 4. The fitting error is defined as

$$\frac{\Delta\rho}{\rho}\% = \left(\frac{\rho_{obs}(T) - \rho_{cal}(T)}{\rho_{obs}(T)}\right) \times 100. \tag{3}$$

We have used two approaches to $f(T)$. In one approach we used a single $f(T)$ over the whole temperature range. For this we have used different types of Debye integral [15] assuming that the temperature-dependent term $f(T)$ arises from electron–phonon interaction. In the other approach we used different $f(T)$ for high-temperature ($T > 100$ K) and low-temperature ($T < 50$ K) regions. The Debye integrals for obtaining the different forms of $f(T)$ have the general form

$$f_n(T) = \left(\frac{T}{\theta_R}\right)^n \int_0^{\theta_R/T} \frac{x^n}{(e^x - 1)(1 - e^{-x})}. \tag{4}$$

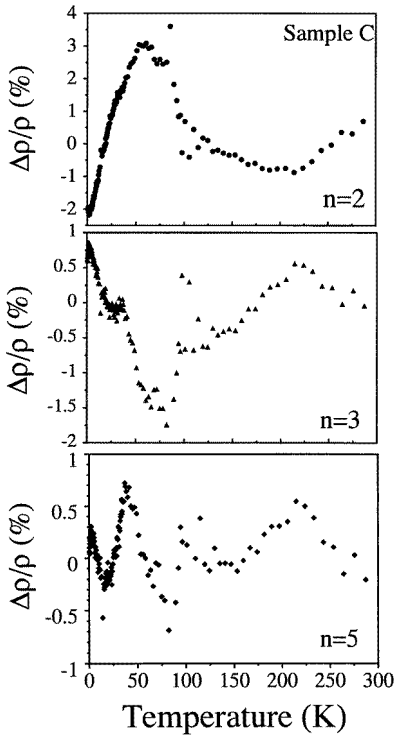

Figure 5. The fitting errors (defined by equation (3)) as a function of temperature for sample C. The fitting errors are for different values of n in equation (4). The error is much less for $n = 5$ compared to that for $n = 3$ or 2.

The advantage of equation (4) is that the single function gives a T^n-dependence at low T ($T \ll \theta_R$) and a linear dependence at $T > \theta_R/2$ irrespective of the value of n. Here θ_R is the characteristic temperature. If $f_n(T)$ does indeed arise from electron–phonon interaction, then θ_R will be comparable to the Debye temperature θ_D obtained from the specific heat. The results are given in table 3 along with the value of n used in the fitting. As shown in figures 4 and 5, for the least resistive sample C, the best fit was obtained with $n = 5$, which is the Bloch–Grüneisen law. Figure 5 is a representative example of the typical temperature dependence of the fitting error. It can be seen that when $f(T)$ is described by the Bloch–Grüneisen law ($n = 5$) the fitting error is less than $\pm 0.5\%$ over the whole temperature range and there is no systematic deviation. For sample B, $n = 3$ and $n = 5$ give comparable fits. The coefficient α which measures the strength of the $T^{1.5}$-term does not seem to show a strong dependence on δ. However, the temperature-independent term ρ_0 and the coefficient β show profound changes as δ changes.

In the second approach we have analysed the resistivity in two separate temperature regions using the form

$$f(T) = \beta' T^m \tag{5}$$

with $m = 1$ for $T > 100$ K and $m = 2$ for $T < 50$ K. We find that this approach gives a better fit. This is mainly because the fitting has been carried out with fewer constraints. The results are given in table 4. A representative example for the relative contribution of the temperature-dependent term obtained using this approach is shown in figure 6 for sample C.

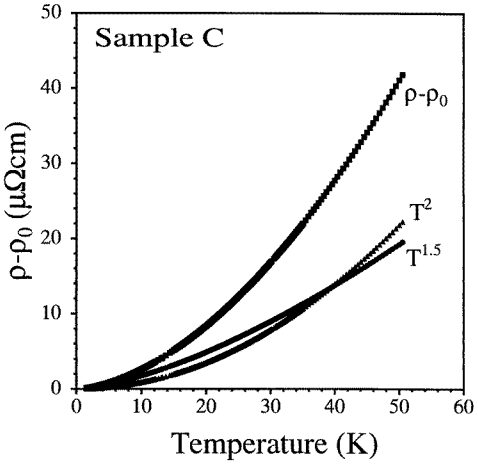

Figure 6. The relative contributions of the temperature-dependent terms ($T^{1.5}$ and T^2) for sample C for $T \leqslant 50$ K. The fitting results are given in table 4.

For sample A at low temperatures ($T < 50$ K), we have the existence of the resistivity minima, and $\rho(T)$ for $T < T_{min}$ shows a shallow rise. We find that the rise of ρ below T_{min} can be best accounted for by using expressions for weak localization (WL). That weak localization is the origin of the rise of ρ below T_{min} is supported by magnetoresistance (MR) measurements (the MR measurements were done on all of the samples and the results will be published elsewhere [16]). The WL contribution to $\rho(T)$ is absent for the less resistive samples. A lack of oxygen stoichiometry ($\delta \neq 0$) introduces localization as has been discussed before. We quantify the weak-localization [14] contribution by means of an additional term $-\gamma T^{0.75}$ which is incorporated into equation (2). Thus, we fit the resistivity below 50 K for sample A using the expression

$$\rho = \rho_0 - \gamma T^{0.75} + \alpha T^{1.5} + \beta f(T). \tag{6}$$

For samples B and C, $\gamma = 0$. For the highly resistive sample A we did not get any meaningful parameters from the fit using the above $f(T)$ given in equation (4) with $n = 3$ and 5. The fit was best with $n = 2$ as shown in figure 7.

The important results of the fits are summarized as follows.

(i) The presence of a $T^{1.5}$-term is necessary but not sufficient for obtaining a good fit. Another extra term, $f(T)$, with a temperature variation faster than $T^{1.5}$ at low temperature is needed. The main difference in the magnitudes of the temperature dependence of the resistivities as seen for different samples comes from the contribution of the term $f(T)$. This is because the contribution of the $T^{1.5}$-term is more or less the same for all of the samples.

(ii) Within the uncertainty of the fit ($\pm 0.5\%$) it is difficult to reach a conclusion on whether there is a T^2-term present in $\rho(T)$. Even if it is present, the coefficient is a sensitive function of δ and increases rapidly as δ increases (see table 3 and sample A). One should not therefore attribute any intrinsic meaning to it and its existence may well be related to oxygen defects (i.e. $\delta \neq 0$).

(iii) The coefficient of the $T^{1.5}$-term does not show much variation when different $f(T)$ are used. Also the value of α does not vary much from one sample to another and is typically 100–150 nΩ cm $K^{-1.5}$. We thus think that the estimate of $T^{1.5}$ is essentially correct. The

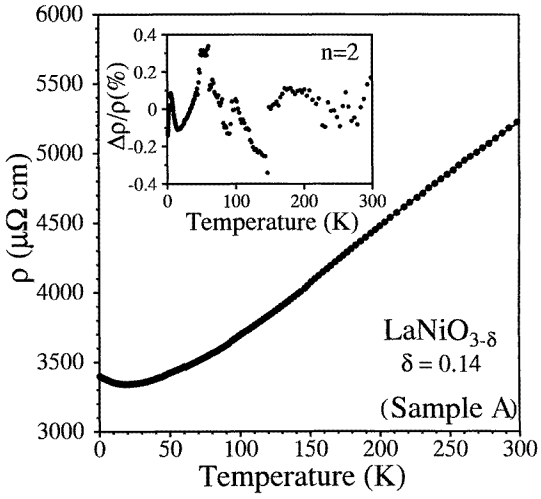

Figure 7. A fit to the resistivity data for sample A. The line is the fit obtained using equations (4) and (6) with $n = 2$. Inset: the fitting error as a function of temperature.

$T^{1.5}$-dependence of the resistivity has been observed for quite a number of transition metal oxides over a wide range of temperatures [17]. It should be noted that the $LaNiO_3$ film (see figure 1) shows a $T^{1.5}$-dependence over the entire temperature region. Although the exact origin of this temperature dependence is not known, we would like to suggest that the origin of this term may be localized spin fluctuations [18, 19], similar to those seen in dilute magnetic alloys such as Cu:**Mn** and Au:**Fe**. In $LaNiO_{3-\delta}$ these spin fluctuations arise due to the formation of localized moments, as the oxygen deficiency creates divalent Ni^{2+}. It has been stated before that the formation of a sufficient amount of Ni^{2+} leads to an insulating state [20]. Close to the composition for which the insulating state occurs ($\delta \approx 0.3$), one finds the onset of spin clusters [21]. We suspect that at lower values of δ one may not have the formation of large spin clusters, but there may exist localized (incoherent) spin fluctuations of the size of a few electronic mean free paths which can give rise to this $T^{1.5}$-term. In metallic alloys the magnitude of the α-term is typically in the range 8–16 nΩ cm $K^{-1.5}$, about one order of magnitude less than that seen for $LaNiO_3$. The strength of the α-term depends on various parameters and is given by [19]

$$\alpha \propto \frac{\Gamma}{n_e} D^2 \left(\frac{JS}{\Gamma}\right)^2 \tilde{a}^6 \left(\frac{k_B}{\Lambda}\right)^{3/2} \tag{7}$$

where: n_e is the carrier concentration; Γ is the conduction bandwidth; D is the ratio of virtual bound states $\pm$ the displacement from the Fermi level to the width parameter; J is the spin–spin coupling constant; S is the spin; $\tilde{a}$ is the lattice parameter; and Λ is the spin-diffusion constant. A combination of low bandwidth Γ and low spin-diffusion constant Λ thus can explain the order of magnitude of the α-term. In view of the various uncertainties involved in estimating α, we think that the magnitude of α observed by us seems to be physically meaningful if we assign it as arising from spin fluctuations. For metallic alloys, α being small, the $T^{1.5}$-term is perceptible only at low T. Unlike for metallic alloys, for oxides the $T^{1.5}$-term is observed over the whole range. However, we stress that at present it is difficult to rule out any other physically plausible mechanism which may give rise to a $T^{1.5}$-term in the resistivity.

3.3. The Ni^{2+} concentration and the magnetic susceptibility

The magnetic susceptibility χ for sample A is shown in figure 8. The susceptibility is higher by nearly a factor of 4 than the previous reported values [5, 6] which were obtained for samples of oxygen stoichiometry comparable to that of samples B and C.

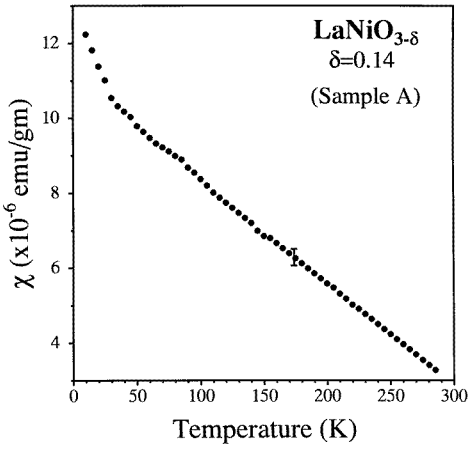

Figure 8. The susceptibility of sample A as a function of temperature.

The higher value of the susceptibility indicates the formation of magnetic moments in the system. We estimate the concentration of the magnetic ions in the system using the χ-data. For $T < 100$ K we have fitted the susceptibility data to the expression $\chi = \chi_0 + C/(T+\theta)$, where χ_0 is the temperature-independent contribution, θ is the Curie–Weiss temperature and C is the Curie constant. A least-squares fit of the data with the above expression gives $\chi_0 = 5.95\times10^{-6}$ emu g^{-1}, $\theta = -51.12$ K and $C = 3.83\times10^{-4}$ emu K g^{-1}. The large value of C can arise from the Ni^{2+} formation as δ increases. For sample A, for which $\delta = 0.14$, about 30% of the Ni in the system is in the Ni^{2+} state. We have estimated the amount of Ni^{2+} contributing to the susceptibility from the value of C obtained from the fit in the following way. In the octahedral coordination, of the eight electrons of Ni^{2+}, six are spin paired in the crystal-field-split t_{2g} levels and two are in the e_g levels and are unpaired. This gives a moment of $S = 1$ for the octahedral coordination. In contrast, in the square-planar coordination there are no unpaired electrons. The eight electrons of the Ni^{2+} pair up to fill four orbitals of the five available 3d levels [22]. This leads to a net moment $S = 0$. Hence for octahedral coordination, considering that the orbital angular momentum is quenched, we get $p_{eff} = g\sqrt{J(J+1)} = 2.83$. This is close to but somewhat lower than $p_{eff} = 3.2$ found for Ni^{2+} in octahedral coordination. Using this value, we estimate the concentration of Ni^{2+} to be about 7×10^{20} cm^{-3} which is only about 4.5% of the total Ni in the system. This is much less than the concentration of Ni^{2+} calculated using δ. Considering the fact that the Ni^{2+} in square-planar coordination makes only a diamagnetic contribution to the susceptibility (due to all of the electrons being paired up), only those Ni^{2+} atoms which are still in octahedral coordination contribute to the susceptibility. Thus the susceptibility gives a clear indication of the formation of square-planar-coordinated Ni^{2+} as δ increases, supporting the argument given in section 3.2.

Earlier reports [5, 6] on the susceptibility of this system have attributed the increase of χ at low temperatures to correlation effects. The value of the Curie constant C obtained

by these prior studies is nearly an order of magnitude less than ours. From reference [6] we get $N = 2 \times 10^{19}$ cm^{-3} assuming p_{eff} to be 3.2. This is less than 0.1% of the total number of Ni atoms in the system. Caution thus needs to be exercised in interpreting the increase in χ as T is lowered below 100 K as arising from correlation effects alone. The values of χ_0 reported in references [5, 6] are also much less (by a factor of 3) than what we find. The Ni^{2+} ions which are in square-planar coordination have $J = 0$ since all of the electrons are paired up. This may give rise to an enhanced temperature-independent Van Vleck paramagnetic contribution leading to a large χ_0.

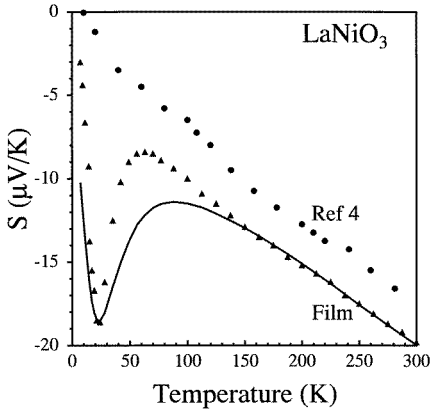

Figure 9. The thermopower of the $LaNiO_3$ film as a function of temperature. Data from reference [4] are plotted for comparison. The solid line is the fit to the data using equation (10).

3.4. The thermopower and the Hall coefficient

In figure 9 we show the thermopower (the Seebeck coefficient S) for a ceramic sample as well as for a film. S is negative over the complete temperature range of 300 K to 10 K. (The resistivity data for the film are shown in figure 1.)

For well oxygenated samples (i.e., for low values of δ) the magnitude of the thermopower at 300 K typically lies in the range -15 to -20 μV K^{-1}, with a linear slope ($|\mathrm{d}S/\mathrm{d}T| \approx$ 0.04–0.05 μV K^{-2}) which seems to be somewhat insensitive to the value of δ. (There is a large negative peak in S for the film at $T \approx 20$ K. We will discuss this issue later on.) The thermopower of $LaNiO_3$ is therefore like that of a metal with electron-like carriers. In the limit of a single dominant carrier we have

$$S = -\frac{\pi^2}{3}\frac{k_B^2 T}{e}\left[\frac{\partial \ln N(E)}{\partial E}\right]_{E=E_F} \tag{8}$$

where $N(E)$ is the density of states. For electrons, e being negative, negative S would imply a negative $\partial \ln N(E)/\partial E$.

From equation (8),

$$\left|\frac{\mathrm{d}S}{\mathrm{d}T}\right| = \frac{\pi^2}{3}\frac{k_B^2}{e}\left[\frac{\partial \ln N(E)}{\partial E}\right]_{E=E_F}. \tag{9}$$

We can obtain an estimate of the magnitude of the thermopower from recent band-structure calculations [23]. We find that $\partial \ln N/\partial E$ is indeed negative, which is in agreement with the observed negative sign of S. From the band structure we estimate

$\partial \ln N/\partial E \approx -4.6$ eV^{-1}. From equation (9) we find $|\mathrm{d}S/\mathrm{d}T| \approx 0.1$ μV K^{-2}. This is slightly larger than the value obtained experimentally (by a factor of 2).

The peak at low temperatures seen for the film deserves comment. This type of peak in S has also been observed recently for closely related materials such as La–Ca–Mn–O and La–Sr–Mn–O [24]. Such peaks can arise if there exists a scattering mechanism from very low-lying excitations. We model these low-lying excitations as a two-level system (TLS) with an energy gap (Δ). For this system, the total thermopower is given as [25]

$$S = -\frac{M}{|e|}\frac{\Delta}{2k_BT}\tanh\left[\frac{\Delta}{2k_BT}[1 + \mathrm{Im}\,\psi(\Delta/2k_BT)]\right] + \eta T \tag{10}$$

where the term ηT is the linear thermopower contribution from equation (8). M is the square of the scattering matrix and thus is a measure of the scattering process, Δ is the splitting of the TLS and ψ is the derivative of the digamma function. A reasonable fit can be obtained for the data with $\Delta \approx 90$ K and $\eta = -0.053$ (shown as a solid line in figure 9). There may be other contributions to the thermopower at low temperature, such as the phonon drag, but essentially the fit shows that the existence of such low-lying excitations can explain phenomenologically the features at low temperatures. However, we cannot offer a firm explanation for the origin of this low-lying excitation at this stage, nor can we explain why it is seen more prominently in films and not in the bulk samples which show comparable values of ρ. It is likely that such low-lying excitations can arise from local rhombohedral distortions of the cubic structure which affect the electron hopping integral by changing the Ni–O–Ni bond angle. This can cause small perturbations in the energy levels varying from site to site. This distortion depends on the local strain which may be different in the film (grown by laser ablation on a substrate) and in well annealed bulk materials. Often a hump in the thermopower is taken as a sign of a phonon drag contribution. We are somewhat reluctant to make this identification for the observed data, for the following reason. A phonon drag requires that the thermal equilibrium is restored within the electronic system mainly by collisions with phonons, and the electron–phonon scattering rate dominates over other scattering rates. In a material like ours with such a small mean free path, the electron–phonon scattering is not the dominant scattering. As a result the phonon drag contribution, if there is one, will be very small.

The Hall coefficient (R_H) has not been measured before. In figure 10 we show the Hall coefficient measured in a field of 6 T as a function of temperature.

This measurement was carried out on the same film for which the thermopower was measured. The sign of the Hall coefficient is positive. It is fairly temperature independent with $R_H \approx 3 \times 10^{-10}$ m^3 C^{-1} implying a carrier concentration $\approx 2 \times 10^{28}$ m^{-3} which is very close to the estimate of the carrier concentration based on the assumption that each formula unit contributes one free carrier. The observed Hall coefficient, however, has a positive sign which is opposite to what one would expect naively from the sign of the thermopower. In addition, at low temperatures ($T < 75$ K) R_H is no longer independent of temperature and it rises as T is decreased. The increase in R_H at low T is very similar to that observed for some metals at low temperatures. As suggested by the free-electron picture, the increase can arise due to the anisotropy in the scattering time on the Fermi surface [26]. In addition, the increase at low temperatures may also mean that some of the carriers are becoming localized due to the disorder arising from oxygen defects. A temperature dependence may also arise from more complex effects as in the cuprate superconductors.

We explain the positive sign of the Hall coefficient as arising from the charge transfer which takes place from the oxygen p band to the metal d band. It has been shown recently that in materials like $LaNiO_3$, the non-bonding oxygen orbitals overlap substantially with

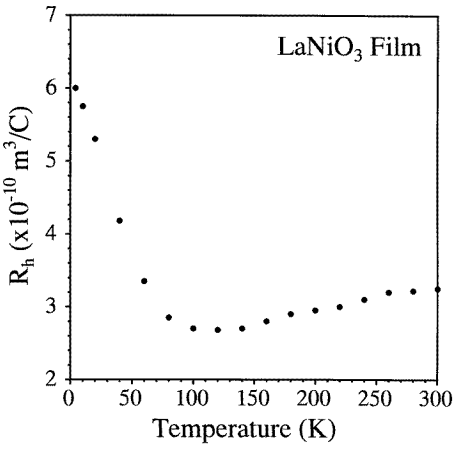

Figure 10. The Hall coefficient as a function of temperature for $LaNiO_3$ film prepared by laser ablation.

anti-bonding metal d orbitals. This gives rise to charge transfer from the ligands to the cations [2]. This will create hole-like pockets in the bands with predominantly oxygen p character leading to a positive contribution to R_H. The charge transfer creates mixed types of carrier in these oxides. It is not clear, however, why the positive contribution to R_H will dominate and will be nearly equal to the free-carrier estimate.

4. Concluding remarks

In this paper we have reported a detailed systematic investigation of the electronic transport in the system $LaNiO_{3-\delta}$. We have attempted to be quantitative in our approach and have established the critical role played by the oxygen stoichiometry. We have also presented results on the Hall coefficient which have not been reported before. In addition, we have also made an interesting observation that while the thermopower is like that of a metallic solid, with negative sign, the Hall coefficient has a positive sign.

Acknowledgments

One of us (AKR) wishes to thank the Department of Science and Technology, Government of India, for a sponsored project. NG wants to thank the Council for Scientific and Industrial Research for a fellowship. RLG acknowledges the support provided by the NSF under Grant No DMR9510475.

References

[1] Raychaudhuri A K 1995 *Adv. Phys.* **44** 21 and references cited therein
[2] Zaanen A, Sawatzky G A and Allen J W 1985 *Phys. Rev. Lett.* **55** 418
[3] Vasanthacharya N Y, Ganguly P, Goodenough J B and Rao C N R 1984 *J. Phys. C: Solid State Phys.* **17** 2745
[4] Rajeev K P, Shivashankar G V and Raychaudhuri A K 1991 *Solid State Commun.* **79** 591
[5] Sreedhar K, Honig J M, Darwin M, McElfresh M, Shand P M, Xu J, Crooker B C and Spalek J 1993 *Phys. Rev.* B **46** 4382

[6] Xu X Q, Peng J L, Li Z Y, Ju H L and Greene R L 1993 *Phys. Rev.* B **48** 1112
[7] Sánchez R D, Causa M T, Caneiro A, Butera A, Vallet-Regi M, Sayagués M Y, Gonález-Calbet J M, Garcá-Sanz F and Rivas J 1996 *Phys. Rev.* B **54** 16 574
[8] Obradors X, Paulius L M, Maple M B, Torrance J B, Nazzal A L, Fontcuberta J and Granados X 1993 *Phys. Rev.* B **47** 12 353
[9] Canfield P C, Thompson J D, Cheong S W and Rapp L W 1993 *Phys. Rev.* B **47** 12 357
[10] Bringley J F, Scott B A, La Placa S J, McGuire T T, Mehran F, McElfresh M W and Cox D E 1993 *Phys. Rev.* B **47** 15 269
[11] Satyalakshmi K M, Mallya R M, Ramanathan K V, Wu X D, Brainard K, Gautier D C, Vasanthacharya N Y and Hegde M S 1993 *Appl. Phys. Lett.* **62** 1233
[12] Sayagués M Y, Vallet-Regi M, Caneiro A and Gonález-Calbet J M 1994 *J. Solid State Chem.* **110** 295
[13] Ganguly P, Vasanthacharya N Y, Rao C N R and Edwards P P 1984 *J. Solid State Chem.* **54** 400
[14] Lee P A and Ramakrishnan T V 1985 *Rev. Mod. Phys.* **57** 287
[15] Ziman J M 1962 *Electrons and Phonons* (Oxford: Clarendon)
[16] Gayathri N, Raychaudhuri A K, Xu X Q, Peng J L and Greene R L 1997 *Phys. Rev.* B submitted
[17] Takagi H, Batlogg B, Kao H L, Kwo J, Cava R J, Krajewski J J and Peck W F Jr 1992 *Phys. Rev. Lett.* **69** 2975
Inaba F, Arima T, Ishikawa T, Katsufuji T and Tokura Y 1995 *Phys. Rev.* B **52** R2221
[18] Rivier N and Adkins K 1975 *J. Phys. F: Met. Phys.* **5** 1745
[19] Ford P J and Mydosh J A 1976 *Phys. Rev.* B **14** 2057
[20] Sreedhar K, McElfresh M, Perry D, Kim D, Metcalf P and Honig J M 1994 *J. Solid State Chem.* **100** 208
[21] Okajima Y, Kohn K and Siratori K 1995 *J. Magn. Magn. Mater.* **140–144** 2149
[22] Pauling L 1993 *The Nature of the Chemical Bond* (Oxford: Oxford University Press and IBH)
[23] Sarma D D, Shanthi N and Mahadevan P 1994 *J. Phys.: Condens. Matter* **6** 10 467
[24] Mahendiran R, Tiwary S K and Raychaudhuri A K 1996 *Solid State Commun.* **98** 701
[25] Fulde P 1984 *Moment Formation in Solids* ed W J L Buyers (New York: Plenum)
[26] Dugdale J S 1977 *Electrical Properties of Metals and Alloys* (London: Edward Arnold)